

STUDY OF MODELLING SPRAY PENETRATION OF BIODISEL FUEL UNDER TRANSIENT ENGINE CONDITIONS

Ahmed Abed Al-Kadhem Majhool, Abbas Alwi Sakhir ALJeebori

Mechanical Engineering Department,
College of Engineering, Al-QadissiyaUniversity,
IRAQ.

ABSTRACT

In this study, numerical investigations are conducted for biodiesel spray under transient engine conditions. The spray tip penetration of biodiesel has been studied in a comparison with diesel fuel in a diesel engine under transient engine conditions. The predicted results are compared with experimental data with a chosen case for highly ambient pressure. The study uses the Eulerian-Eulerian approach for the two phase flow simulation. In the validated computer programme both used liquid fuels are treated in terms of spray moments of drop size distribution. One parameter is selected for the analysis and to study the spray characteristics through the examination and tracking the behavior of the biodiesel. The obtained results for biodiesel fuel and diesel fuel of the spray tip penetration show a good agreement with the experimental results.

Keywords: Two-phase flow, spray moment method ,biodiesel , diesel, spray penetration

INTRODUCTION

The common understanding of the necessity to use a clean, biodegradable and renewable fuel as alternative fuel has led to present the biodiesel as outstanding solution for the energy security and environment problems. During the last two decades , a big effort has been spent on the effect of alternative fuel properties. In the same way, biodiesel can improve the thermal efficiency through the optimum combustion process and reduced exhaust emission characteristics of diesel engine which is elected by fuel properties and spray atomization characteristics .Applicative research based on using different biofuels expressed that the fuel with higher density, viscosity and surface tension gives shorter spray tip penetration and large cone angle (Kusak *et al.*, 2002; Lee *et al.*, 2005; Wengian, 2006; Allen, 1998; Yamane & Shimamoto, 2001).

Experimental and theoretical study to the characteristics of an undiluted biodiesel fuel were made by Park *et al.* (2009). Their investigation were led to when the injection pressure increased the injection delay time decreased due to the increase in spray injection velocity. They used KIVA-3V code to perform the numerical calculations. The results of spray tip penetration for biodiesel has similar trend as it compared with diesel fuel at different injection and ambient conditions.

The impact of various fuel temperature and ambient gas conditions were studied by (Park *et al.*, 2009). In their experimental and numerical work, they found that the spraytip penetration has the same pattern in spite of the different in fuel properties due to the change in fuel temperature.

An experimental and numerical calculations have been performed by (Xiangang *et al.*, 2010). They used the light scattering technique to measure non-evaporating spray of diesel and two biodiesel under high injection pressure up to 300 MPa. The obtained results were showed that the biodiesel fuel gives longer injected delay time and spray tip penetration while the cone angle is smaller compared with the diesel fuel. Also, they confirm that the physical properties of biodiesel affected on spray atomization processes significantly.

A FLUENT v6.3 and CONVERGE code were implemented by (Som *et al.*, 2010) to simulate a comparison for the behavior of spray under ambient and evaporation conditions of biodiesel with petrodiesel fuel. The predicted results showed that the biodiesel fuel has poor atomization characteristics compared to diesel fuel. The spray tip penetration and SMD were found higher where as smaller cone angle was obtained for biodiesel.

The Two Phase Model

Spraymomentstheory

Beck and Watkins (2003) presented their approach based on the droplet number size distribution, $n(r)$, is defined as a multiple of the droplet number probability distribution of droplet radius as below

$$n(r) = \int_{r_m^{in}}^{r_m^{ax}} N(r) dr \quad (1)$$

where ($N(r)$) is the droplet number probability distribution. The integral over all droplets provides the total number of droplets per unit total volume (not unit liquid volume). This can be defined as below:

$$Q_0 = \int_0^{\infty} n(r) dr \quad (2)$$

This is the first moment of the distribution function. In this approach, the three remaining distribution function moments are defined as below:)

$$Q_i = \int_0^{\infty} r^i n(r) dr \quad (3)$$

At a particular point in space and time, Q_0 is the total number of drops present, Q_1 is the total sum of radii of the drops, $4\pi Q_2$ is the total surface area of the drops and $4\pi Q_3/3$ is the total volume of the drops, all quantities within a unit volume of the gas/liquid mixture. The fourth moment is related to the liquid volume fraction via the following relation

$$\frac{V_{Liquid}}{V_{Liquid} + V_{gas}} = \frac{4\pi}{3} Q_3 = 1 - \Theta \quad (4)$$

where Θ is the gas volume fraction. Furthermore, these four parameters provide all mean droplet diameters from D_{10} to the Sauter mean diameter D_{32} , as, by definition,

$$D_{pq}^{p-q} = \frac{2^{p-q} Q_p}{Q_q} \quad (5)$$

Liquid-phasetransportequations

The transport equation for the fourth droplet moment is effectively a liquid-phase continuity equation. To derive the equation, first consider an equation for a group of droplets with similar properties as would be solved in a multi-size Eulerian treatment; thus, for a droplet group occupying volume fraction k ,

$$\frac{\partial}{\partial t} (\rho_i \gamma_k) + \frac{\partial}{\partial x} (\rho_i \gamma U_{Lkj}) = -S_{mk} \quad (6)$$

where S_{mk} is the mass transferred from this group of droplets to the gas phase per unit volume. Density is denoted by ρ , velocity by U and the subscript L indicates liquid phase. This equation can be re-expressed in terms of the number (n_k) and

radius (r_k) of the droplets in this group as

$$\frac{4}{3}\pi \frac{\partial}{\partial t}(\rho_l n_k r_k^3) + \frac{4}{3}\pi \frac{\partial}{\partial x}(\rho_l n_k r_k^3 U_{lkj}) = -S_{mk} \quad (7)$$

Now, allowing the number of droplets in each group to become small, and summing over all groups (effectively all droplets), the equation becomes

$$\frac{4}{3}\pi \frac{\partial}{\partial t} \left(\int_0^\infty \rho_l n(r) r^3 dr \right) + \frac{4}{3}\pi \frac{\partial}{\partial x} \left(\int_0^\infty \rho_l n(r) r^3 U_{ij} dr \right) = -S_{mk} \quad (8)$$

which can be written as

$$\frac{4}{3}\pi \frac{\partial}{\partial t}(\rho_l Q_3) + \frac{4}{3}\pi \frac{\partial}{\partial x}(\rho_l Q_3 U_{lkj}) = -S_{mk} \quad (9)$$

and then, in terms of the liquid-volume fraction, $1 - \Theta$, as

$$\frac{\partial}{\partial t}(\rho_l(1 - \Theta)) + \frac{\partial}{\partial x}(\rho_l(1 - \Theta)U_{lkj}) = -S_{mk} \quad (10)$$

The convection velocity required is thus seen to be the expected moment-average value (denoted by subscript 3), and the equation clearly represents a liquid-phase continuity equation. The source term has only one contribution due to evaporation, as the other phenomena considered do not affect the total mass of liquid present. That equations for the remaining moments take a similar form, but more care must be taken as more source terms arise due to the changes effect By droplet breakup, droplet collisions, evaporation and changes in the droplet density. The equations are

$$\frac{\partial}{\partial t}(Q_i) + \frac{\partial}{\partial x}(Q_i U_{ij}) = -S_{Q_i} \quad (11)$$

Use of the i th moment-average velocity in the equation should be noted. The liquid mass-average velocity, or liquid momentum equation, as employed in the calculation scheme, is based on the work of (Harlow & Amsden, 1975) for particulate flows. Equation (11) is derived starting from the Lagrangian form of the equation for a group of droplets with identical properties, and the details of derivation of this equation appeared in (Beck & Watkins, 2003a). In brief, the liquid phase momentum equation is written as

$$\begin{aligned} & \frac{\partial}{\partial t}(\rho_l(1 - \Theta)U_{13i}) + \frac{\partial}{\partial x_j}(\rho_l(1 - \Theta)U_{13i}U_{13j}) + U_{13i}S_m \\ & = \frac{\partial}{\partial x_j}(\rho_l(1 - \Theta)\sigma_v \nu_l (\frac{\partial U_{13i}}{\partial x_j} + \frac{\partial U_{L3j}}{\partial x_i})) - S_{U_i} \end{aligned} \quad (12)$$

Where is ρ_v the coefficient of [Melville and Bray, 1979], ν_l is the turbulent equivalent viscosity, m and U_i are the source terms of mass and momentum, respectively. The remaining equations for the moment-average velocity are derived in a similar manner as described by (Beck & Watkins 2003a). Thus

$$\begin{aligned} & \frac{\partial}{\partial t}(Q_k U_{lkj}) + \frac{\partial}{\partial x_j}(Q_k U_{lkj} U_{lki}) + \frac{\partial}{\partial x_j}(Q_k (U_k (U_{13i} - U_{lki})(U_{13j} - U_{lkj}))) + U_{13i} B_{Q_i} + U_{lki} (S_{Q_i} - B_{Q_i}) = \\ & \frac{\partial}{\partial x_j}(Q_k \sigma_v \nu_l (\frac{\partial U_i}{\partial x_j} + \frac{\partial U_j}{\partial x_i})) - S_{U_{lki}} \end{aligned} \quad (13)$$

Gas-phase transport equations

The gaseous transport equations employed are in standard form. These are given in full in (Beck & Watkins, 2003a). The turbulence model employed is a two-equation model, the equations being solved for the turbulence kinetic energy k , and its dissipation rate ϵ . The $k - \epsilon$ turbulence model has been used extensively for single-phase simulations of turbulent flows for many years. It has also been incorporated into the majority of schemes for two-phase spray simulations (see, for example, the KIVA computer codes (Amsden *et al.*, 1989). The spray simulations presented in this paper are of simple shear flows. The $k - \epsilon$ [Launder and Spalding, 1972] model is therefore appropriate, since it is particularly developed for such flow situations. It is intended that more advanced turbulence models will be incorporated into the current spray methodology in the near future. The calculation of the gaseous turbulent viscosity through the turbulence model is, as mentioned above, also used to evaluate the liquid-phase turbulent diffusion, through the model of (Mostafa & Mongia, 1987). The gas and liquid phases also interact through the source terms in the continuity, momentum and heat transfer equations. All the source terms in the gas-phase equations are calculated by considering the effect of the gas phase on the liquid phase in terms of the droplet-size-distribution-function moments (Beck & Watkins, 2002, 2003).

Table 1. Physical conditions for the parametric tests and experimental validations [Data of Hiroyasu and Kadota 1974].

	H3
Temperature of Gas (K)	293
Gas Pressure (MPa)	5.0
Gas Density (kg/m ³)	59.46
Spray Angle (degree)	21
Injection Velocity (m/sec)	86.4
Injection Pressure (MPa)	9.9
Nozzle Radius (mm)	0.3
Chamber Length (mm)	95.0
Chamber Radius (mm)	20.0
Injection SMR (μm)	15.0
Time Step (π sec)	2.0
Simulation Time (msec)	2.50

Table 2. Fuel properties of diesel and biodiesel fuels

Fuel properties	Diesel	Biodiesel
Density (288 K) (kg / m^3)	830	885.1
Viscosity (303 K) (mm^2 / s)	3.36	4.45
Surface tension (mN / m)	25.5	25.7

GAMMA DISTRIBUTION

The general gamma number size distribution is given by

$$n(r) = Q_0 \frac{(k-2)^k}{\Gamma(k)r_{32}^k} r^{k-1} e^{-\frac{r}{r_{32}}} \quad (14)$$

And

$$\Gamma(k) = \int_0^{\infty} x^{k-1} e^{-x} dx \tag{15}$$

where $\Gamma(k)$ is the gamma function and r_{32} is the Sauter mean radius of the number size distribution of the drops. This is defined by $r_{32} = Q_3/Q_2$. For numerical calculations, the gamma function can be approximated by [18]:

$$\Gamma(k) = \left(\frac{k}{e} \left(k \sinh \left(\frac{1}{k} + \frac{1}{810^6} \right) \right)^{0.5} \right)^k \left(\frac{2\pi}{k} \right)^{0.5} \tag{16}$$

with an error of at most 1% for values of $k > 10$. The two parameters defining the functional form of the gamma distribution are r_{32} and k . It is clear that a variety of uni-modal distributions can be obtained, ranging from relatively skewed examples when k is small, to essentially symmetric examples for large k . With three moments calculated through transport equations, there are two parameters ($Q_3/Q_2 = r_{32}^2$ and Q_2/Q_1) available to determine r_{32} and k . Insertion of equation (14) into equation (3) and partial integration leads to

$$Q_i = \frac{(k+2)Q_{i+1}}{(k+i)r_{32}} \tag{17}$$

hence, setting $i = 1$,

$$k = \frac{(2Q_r - 1)}{(1 - Q_r)} \tag{18}$$

$$Q_r = \frac{(Q_2^2)}{(Q_1 Q_3)} \tag{19}$$

Q_0 is calculated from equation (17), by setting $i = 0$. The gamma distribution is defined for all $k > 0$. However, in practice there are a number of restrictions that must be applied, arising from the sub-models employed; in particular, the drag and drop break-up and collision models used

TEST CASE

This section discusses the experimental data that carried out by (Hiroyasu & Kadota, 1974) focuses about spray tip penetration and discusses about the effect of injected pressure and density on spray penetration. The operating conditions were selected for the type of narrow solid-cone spray. The chosen test case is 3 of (Hiroyasu & Kadota, 1974) the physical conditions for which are given in table 1. The experimental results given are penetration rates where the penetration data were measured photographically, and this model adopted considers the same variables. Hiroyasu and Kadota (1974) varied out number of experiments on fuel sprays using high pressure diesel engine injection system. The measurements were taken at the room temperature between 293 and 298 for different ambient gaseous pressure ranged from 0.1 MPa to 5 MPa help of the liquid immersion sampling technique with a mixture of water-methylcellulose solution and ethanol utilized as an immersion liquid for diesel oil.

SOLUTION SCHEME

The equations are all solved on the same two-dimensional axisymmetric orthogonal computational grid as shown in **Figure 1**. The collocated grid approach is used, which involves defining a central

control volume for the gas pressure and other scalar variables, including the moments and displaced volumes for the gas and liquid velocities. The temporal differencing is performed using the Three Time Level method which is a second order implicit scheme and has no time step constraint. This is marginally more complex than the Euler scheme and results in a fully implicit scheme that allows larger time steps to be taken before the scheme becomes unstable. This is generally a good idea in the modeling of spray flows, as a fine grid is required around the nozzle region in order to resolve the large dependency on inlet conditions. An explicit scheme, for stability, requires prohibitively small time steps. This is especially the case when considering the large injection velocities of high-pressure diesel sprays and when the very small dimensions of the injector, of $O(10^{-4})\text{m}$, are discretized into a number of injection cells, as done here. Spatial discretization of the velocity equations for both phases and the turbulence model equations is done using the upwind scheme. To enhance the stability of the computational calculations the central differencing scheme is used for moments, vapour mass fraction and energy equations.

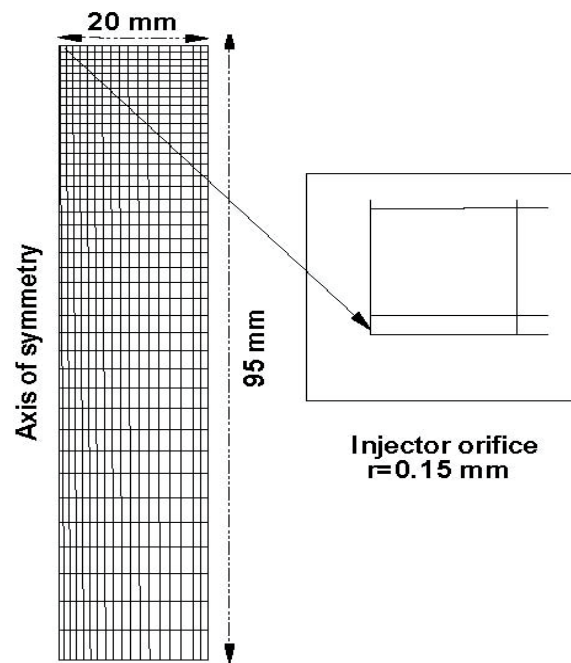


Figure 1. Computational domain

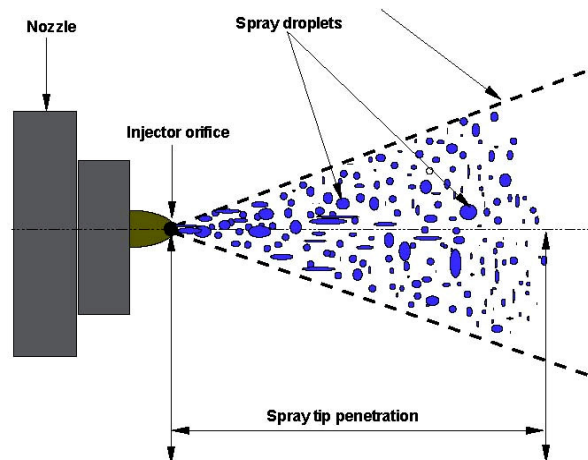


Figure 2. Definition of spray tip penetration

RESULTS AND DISCUSSIONS

In order to validate the present numerical calculations, the spray tip penetration will be chosen as a crucial parameter to be compared with experimental data measured by. The definition of spray tip penetration is the axial distance between the injector orifice to the farthest location can be reached by the spray droplets as shown in **Figure 2**.

In **Figure 3** illustrates the comparison of spray tip penetration of diesel fuel and biodiesel fuel against the experimental data. The experimental spray tip penetration was evaluated by measuring the visible leading edge of spray images. The spray tip penetration was determined in the calculations by using the leading edge from the fourth spray moment. The fourth spray moment was defined as in theoretical section as the volume fraction of the liquid phase. Here, the **Figure 3** is divided into parts (a) and (b) in order to realize the hydrodynamic and ambient effects on the spray type whether the spray is classified as a solid or hollow cone spray. Furthermore, the most important reason described here in this work is the fuel physical properties. For example the fuel density can be affected on the atomization process and spray tip penetration by decelerating the injection delay time. As the density increases it will give sufficient time to breakup into small droplets and the ambient gas will pass through these droplets producing higher drag force. In addition, when the fuel density increase the spray injection velocity (spray momentum) will be reduced normally according the relation that calculates the initial spray value:

$$U_{inj} = cd \sqrt{\frac{2(P_{inj} - P_{amb})}{\rho_{liq}}} \quad (20)$$

Experimental data were concurrently compared with the obtained numerical results, and the spray characteristics of the diesel fuel and biodiesel fuel were compared with those of the diesel fuel. The properties of diesel and biodiesel fuel are shown in Table 1 to be taken from (Xiangang *et al.*, 2010).

Part (a) in **Figure 3** shows that both biodiesel and diesel fuel give over-estimated calculations as compared with experimental data because the start up condition for the nozzle at the begin of injection time upto (0.5 msec). The interval time between (1.0 msec) to (1.5 msec) also recorded over-prediction for the spray tip penetration and the biodiesel fuel shows better results than diesel fuel because it has late injection time due to the higher density. Part (b) in **Figure 3** shows that both biodiesel and diesel give under-estimated results as compared with reference data with an acceptable difference of 15%.

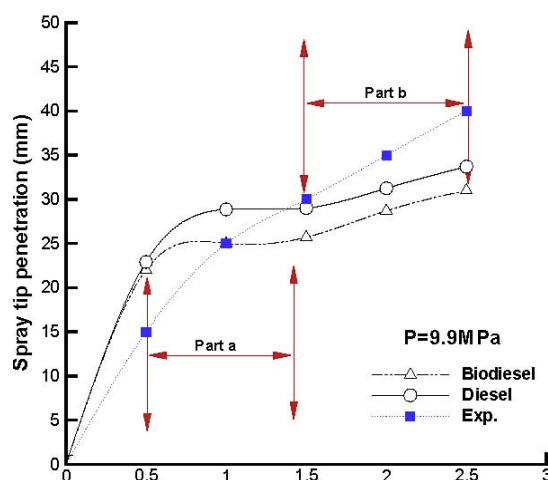


Figure 3. Comparison of predicted spray tip penetration with experimental data.

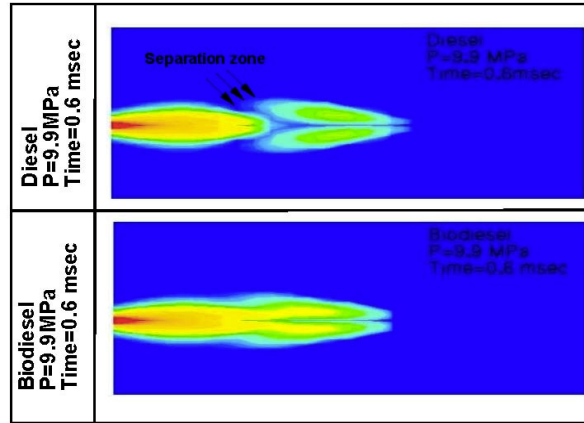


Figure 4. Liquid volume fraction of diesel and biodiesel at time 0.6 msec

Figure 4 shows the contour plot for spray volume fraction (Q3) at time (0.6 msec). The separation zone as pointed in the figure is formed due to the atomization process. It appears clearly in diesel fuel compared to the biodiesel fuel because the low density of diesel of (830 kg/m³). To prove this observation, a repeated results for spray tip penetration are presented in Figure 5.

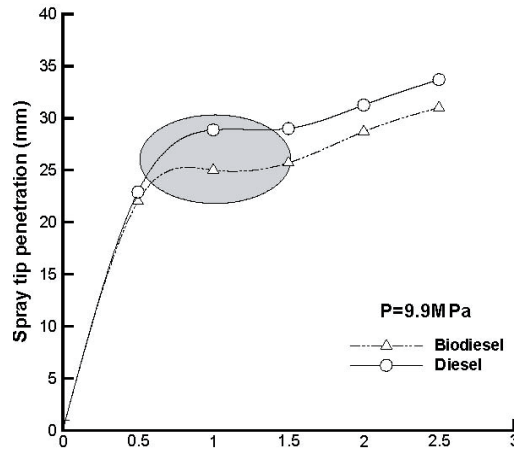


Figure 5. Variation of spray tip penetration with time

The shadow area in Figure 5 is between (0.5 msec) and (1.5 msec). It shows that because of the lower injected delay time and the atomization effect the spray tip penetration is reduced and then gradually rise due to the spray propagation.

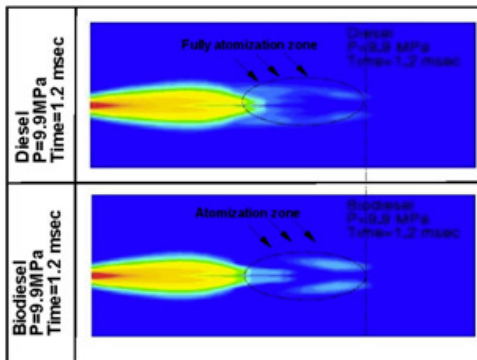


Figure 6. Liquid volume fraction of diesel and biodiesel at time 1.2 msec

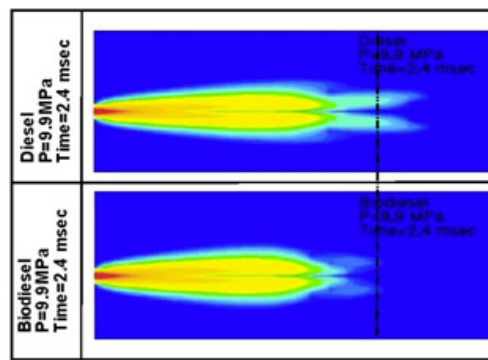


Figure 7. Liquid volume fraction of diesel and biodiesel at time 2.4 msec

Figure 6 shows the fully atomization zone in diesel fuel where as a poor atomization has been recorded for biodiesel fuel. It should be noted that the biodiesel fuel expressed approximately the same spray tip penetration. This is because the dense region in biodiesel which imposes a highly spray momentum are found due to the large mass of injected fuel. This observation has not been seen in **Figure 3** because of the selected points for the comparison are (1.0 msec and 1.5 msec).

Normally trend is retained for biodiesel fuel and diesel fuel has been shown in **Figure 7**, where the diesel fuel offers a higher spray tip penetration than biodiesel fuel as discussed above in part (b) in **Figure 3**. The parameter that have been play important role in these results is the liquid volume fraction (Q3) which is used to determine where the front and the boundary of the spray. Both **Figure 8** and **Figure 9** show the droplets distribution along the body of the spray at random selected time of (1.0 msec) and (2.5 msec) respectively. The highly concentrated droplets are found near the injector orifice because of the accumulation of the injected mass of the liquid. Also the figures describe the reduction in spray volume towards the front of the spray due to the effect of atomization process. From these plots, the spray tip penetration can be evaluated as being the position at any given time where the liquid volume fraction approaches to zero value at the head of the spray as shown in **Figures 8** and (9).

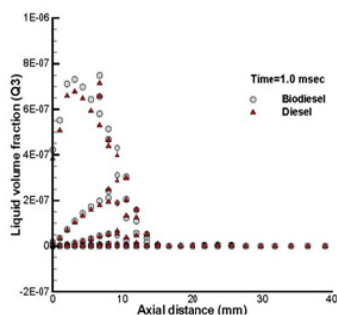


Figure 8: Variation of liquid volume fraction of diesel and biodiesel at time 1.0 msec.

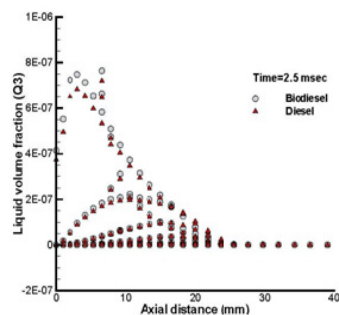


Figure 9: Variation of liquid volume fraction of diesel and biodiesel at time 2.5 msec.

CONCLUSIONS

This paper presents a new numerical study for the biodiesel fuel spray which is implemented in a CFD code to simulate a spray inside a cylinder of diesel engine. The conclusions from the numerical analysis performed in this study is summarized as follows :

1. The biodiesel fuel offers a similar trend for the spray tip penetration but it produces lower values as compared with the diesel and experimental data because it imposes the higher density which tends to reduced the injected velocity.
2. The presented results here are discussed from the view point of the liquid volume fraction for the spray which is sufficient for the spray tip penetration but it is not for the other processes such as atomization (drag, break-up and collision).
3. The study present a controversial results for spray tip penetration which it needs to be studied widely and take more than one parameter such as Sauter mean diameter and Webber number to get a fully picture for the biodiesel behavior.

REFERENCES

- Lee, S., Tanaka, D., Kusaka, J. and Daisho, Y. (2002). Effects of diesel fuel characteristics on spray and combustion in a diesel engine; JSAE200224660, *Japanese Society of Automotive Engineers*: Tokyo, Japan.
- Lee, C.S., Park, S.W. and Kwon, S.I. (2005). An Experimental Study on the Atomization and Combustion Characteristics of Biodiesel-Blended Fuels. *Energy Fuels*, 19, 2201.

- Wengiao, Y. (2006). *Computational modelling of nitrogen oxide Emissions from biodiesel based on accurate fuel properties*. Yuan, W. PhD Dissertation, University of Illinois at UrbanaChampaign. Department of Agricultural and Biological Engineering.
- Allen, C.A.W. (1998). *Prediction of biodiesel fuel atomization characteristics based on measured properties*. PhD Dissertation, Dalhousie University-DALTECH, Halifax, Canada.
- Yamane, K., Ueta, A. and Shimamoto, Y. (2001). *Influence of Physical and Chemical Properties of Biodiesel Fuel on Injection, Combustion and Exhaust Emission Characteristics in a DI-CI Engine*, The Fifth International Symposium on Diagnostics and Modeling of Combustion in IC Engines COMODIA, Nagoya, Japan.
- Park, S.H., Kim, H.J. Suh, H.K. and Lee, C.S. (2009). A study on the fuel injection and atomization characteristics of soybean oil methyl ester (SME). *International Journal of Heat and Fluid Flow*, 30, 108–116.
- Park, S.H., Kim, H.J. Suh, H.K. and Lee, C.S. (2009). Experimental and numerical analysis of spray-atomization characteristics of biodiesel fuel in various fuel and ambient temperatures conditions. *International Journal of Heat and Fluid Flow*, 30, 960970.
- Wang, X., Huang, Z., Kuti, O.A., Zhang, W. and Nishida, K. (2010). Experimental and analytical study on biodiesel and diesel spray characteristics under ultra-high injection pressure. *International Journal of Heat and Fluid Flow*, 31, 659666.
- Som, S., Longman, D.E., Ramirez, A.I. and Aggarwal, S.K. (2010). *A comparison of injector flow and spray characteristics of biodiesel with petrodiesel*. Fuel, 89, 40144024.
- Beck, J.C. and Watkins, A.P. (2003). On the development of a spray model based on drop-size moments. *Proc. R. Soc. Lond.*, A(459), 1365-1394.
- Harlow, F.H. and Amsden, A.A. (1975). Numerical calculation of multiphase fluid flow. *Journal of Computational Physics*. 17, 19–52.
- Beck, J.C. and Watkins, A.P. (2003a). On the development of a spray model based on drop-size moments. *Proc. R. Soc. Lond.*, A(459):13651394.
- Melville, W.K. and Bray, K.N.C. (1979). A model of the two-phase turbulent jet *International Journal of Heat and Mass Transfer* v.22, 647–656 .
- Beck, J.C. and Watkins, A.P. (2003). The droplet number moments approach to spray modelling: The development of heat and mass transfer sub-models. *Int. J. of Heat and Fluid Flow*, 24, 242-259.
- Amsden, A.A., O'Rourke, P.J. and Butler, T.D. (1989). *KIVA-II: A computer program for chemically reactive flows with sprays*, Technical Report LA-11560-MS, Los Alamos National Laboratory.
- Launder, B.E. and Spalding, D.B. (1972). *Mathematical models of turbulence*, London academic press.
- Mostafa, A.A. and Mongia, H.C. (1987). On the modelling of turbulent evaporating sprays: Eulerian versus lagrangian approach. *Int. J. Heat and Mass Transfer*, 30.
- Windschitl, R.H. (Available) <http://www.rskey.org/gamma.htm>.
- Hiroyasu, H. and Kadota, T. (1974). *Fuel droplet size distribution in diesel combustion chamber*. SAE, paper 740715.